

Chapter 2

Structural studies on polyurethane elastomers

2.1 General considerations on the phase separation and morphological features

The whole is more than the sum of its parts (Aristotle)

In addition to chemical interactions, the physical arrangement of the molecules plays an important role.

Remember the widely accepted paradigm that “*the whole is more than the sum of its parts*”? Cumulative effects and interactions in a PU material system reveal more than the parts hidden properties. The reverse is effective as well.

Morphology is defined as *the science of structural forms*. PUs properties originate in their nanoscale phase separation by the competition between the hard and soft phases. PUs morphology can be studied at different levels of structure according to their domain sizes [4]. At an intermediate level a two phase structure is observed, where the dimensions of domains are of the order of 5–100 nm.

It is well-known that the PUs tend to exhibit phase separation where the SS units confer elastomeric behaviour while the microphase rich in HS provides physical cross-linking—see [4, 74, 78, 80, 125–127], for example the review by Dietrich and Hespe [126]. In addition to the microphase separation of segments, the macrophase separation of molecules with different composition has to be considered in discussing the PUs morphology and their properties. As this phenomenon is supposed to be common for PUs, it is also important to study the control and characterization of the heterogeneity of segmented macromolecules and also the relationship between properties and the molecular heterogeneity.

Because of the basic thermodynamic incompatibility of the segments, localized microphase separation occurs, leading to the well recognized domain structure, and the properties of the final bulk material are strongly influenced by the extent of microphase separation and by the morphological characteristics of the domains (Fig. 2.1 and 2.2).

Fig. 2.1 Schematic representation of a well phase segregated PU system

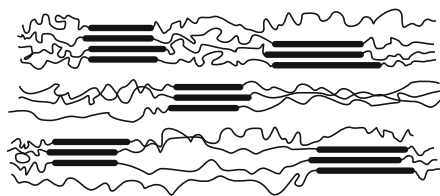


Fig. 2.2 Schematic representation of a phase mixed PU system



It is energetically favourable for the SS and HS not to mix. Thus during cooling from above a critical order-disorder temperature, spontaneous segregation of SS and HS into separate soft (SS-rich) and hard (HS-rich) phases occurs by the process of spinodal decomposition. To achieve elastomeric performance, the SS must be the majority constituent by mass, and the phase structure then takes the form of discrete hard domains dispersed within a soft matrix. Such a phase structure impacts on mechanical properties, and a further structural parameter of importance, therefore, is the *degree of phase separation*.

PU's phase separation strongly depends on the hydrogen bond formation between the urethane linkages, as well as on the manufacturing process, and reaction conditions [4, 128–132]. It also depends on the SS type and molecular weight. As the SS molecular weight decreases, the phase mixing increases [77]. Furthermore, the molecular weight of the SS is a dominant factor since higher molecular weights easily form rich phases on account of entropic contribution. As long as the size of the microphase-separated structure is of a nanometer scale, PUs can be classified as nanostructured materials [131].

The extent of the hydrogen bonding which is related to the phase separation is affected by the material structure, composition and temperature. In linear PUs, Tiffan and Terenzi found that almost all NH groups at room temperature are hydrogen bonded [132]. Similar observations were made by Boyarchuk et al [133] both for polyether and polyester PUs.

The overall mechanical properties of the material depend upon the relative volume fractions of soft and hard phases, and on the intrinsic properties of each of the phases. These in turn depend on details of molecular packing of the constituents within the phases, including the density of hydrogen bonds.

There is a wide variety of compositional variables which can affect the degree of phase segregation, the organization of the HS and consequently the PU's mechanical properties. The *symmetry of the diisocyanate* is an important factor. For example, Sung et al. studied a series of polymers based on the diisocyanates 2,4-TDI or 2,6-TDI, extended with BDO, and polyether or polyester SS of molar masses 1 000 or 2 000 g/mol. In the 2,4-TDI polymers, the *asymmetric* placement of the isocyanate residues with respect to the methyl group resulted in some head-to-tail

isomerization in the HS. In contrast, in the 2,6-TDI based materials, this problem was absent since the molecule is *symmetrical* [134]. Other compositional variables were undertaken in this study: the macrodiol type (polyether or polyester SS macrodiol), the SS molecular weight and the length of the HS.

All of the 2,4-TDI polymers had amorphous domain structures with HS glass transitions below 100°C, whereas all of the 2,6-TDI based polymers exhibited semicrystalline HS structures with melting temperatures in the range of 130° to 200°C [134]. The interurethane hydrogen bonding was proved to be insufficient in order to stabilize the HS domains and to assure extensive phase segregation. As shown by Sung et al, there were other conditions that also contributed to PUs phase incompatibility such as the increase in the SS molecular weight, and the use of a less polar SS like hydroxy terminated polybutadienes (PBU).

For segmented PUs synthesized with PBU in bulk, Xu et al [21] showed that such materials contain two fractions of segmented macromolecules with quite different composition and average HS length. The morphological complexity of such PUs was interpreted by taking into account the domain formation due to the segregation phenomena on different levels, namely, macrophase separation and microphase separation. The general morphological features observed in the PBU based PUs were useful to understand the morphology-property relationships of other segmented copolymers.

Comparing the effects of polyether and polyester SS, the polyester macrodiol PBA introduced greater phase mixing than the PTMO soft segments, thereby raising the glass transition temperature of the SS [4, 134, 135]. These results confirmed that the hydrogen bonding to ester is stronger than to ether.

There was also evidence that the hydrogen bonding interaction can interfere with the SS crystallization, as long as the SS crystallization did not occur in polymers like those based on 2,4-TDI-PTMO (molar mass 2 000 g/mol), whereas a slight improvement in phase segregation occurred in the polymers with 2,6-TDI-PTMO of molar mass 2 000 g/mol [134]. The SS segment crystallized freely as indicated by a further decrease in the glass transition temperature.

Similar comparisons were made for materials obtained with the diisocyanate MDI by using the polyester PBA of analogous molar mass. The MDI materials showed that hydrogen bond dissociation can occur within an ordered domain structure at temperatures well below the domain transition temperature and with little regard for improvement in the degree of order [134]. The thermal behaviour of hydrogen bonding appeared to be virtually independent of the PUs structural organization.

Previous publications [136, 137] reviewed models proposed for HS achieved with the diisocyanate MDI and extended with BDO. A detailed morphological analysis [137] of a series of such materials showed that the hard microdomain structure was in qualitative agreement with the model proposed by Koberstein and Stein [136]. This model was based on the partial solubilization of short HS into the soft microphase. HS shorter than the critical length for microphase separation were presumed to remain within the soft microphase while longer segments aggregated into lamellar hard microdomains of thickness proportional to the critical sequence

length. Models of this nature provided a means for relating chemical structure and thermodynamics to the PUs properties.

Mc Kiernan [138, 139] studied the influence of the hydrogen bonding on the crystallization behaviour of a series of linear, *aliphatic* m,n-polyurethanes $[\text{O}-(\text{CH}_2)_m-\text{O}-\text{C}(\text{O})-\text{NH}(\text{CH}_2)_n-\text{NHC}(\text{O})]_x$ derived from long chain aliphatic diols. The studies showed that, hydrogen bonding still influenced the crystallization process of the long-chain, aliphatic PUs. The X-ray and electron diffraction, and infrared spectroscopy indicated that long alkane PUs segments have interchain and intersheet distances similar to that observed for PUs of higher hydrogen bonding densities. The hydrogen bonding controls the crystallization, packing, and morphology of such materials. In addition, high-temperature infrared studies showed the existence and high concentration (~75%) of hydrogen bonding in such PUs even in the melt [138, 139].

The three-dimensional hydrogen-bonding ability to act as an additional driving force for more complete phase segregation determines stronger interaction between the HS.

Hydrogen bonding can be detected and studied by means of *IR spectroscopy*. The changing distribution of hydrogen-bonding properties in the hard and soft domains can be assessed by this technique. The hydrogen bonded and free N–H and urethane carbonyl C=O are the peaks of interest [140–148]. PUs phase separation in PUs can be characterized by measuring the intensity and position of the hydrogen-bonded N–H stretching vibration. HS–HS hydrogen bonding ($\text{N}-\text{H}\cdots\text{O}=\text{C}$) in the hard domains and HS–SS ($\text{N}-\text{H}\cdots\text{O}-$) hydrogen bonding in phase-mixed states were identified. In the case of well segregated PUs systems, there is significant $\text{N}-\text{H}\cdots\text{O}=\text{C}$ hydrogen bonding, since both units are associated with the HS. N–H can form strong hydrogen bonding with the oxygen of the ether groups associated with the SS, where observation of the hydrogen bonds indicates the existence of a dispersed phase consisting of HS mixed with SS [149]. In general, the N–H groups free from hydrogen bonding have a stretching vibration at $3\,450\text{ cm}^{-1}$. In contrast, the groups involved in hydrogen bonding have much lower frequencies, ranging from $3\,300$ to as low as $3\,200\text{ cm}^{-1}$. The exact position depends on the strength of the hydrogen bonding. The spectroscopic data can then be correlated to the macroscopic structural transformation, mainly the degree of phase mixing or the separation kinetics.

The extent of hydrogen bonding is affected by the nature of the SS. Eisenbach and Gronski [150] found that 40% of carbonyls in polyether urethanes are hydrogen bonded, which is much less than with polyester urethanes on the same basis but at a higher HS content [151]. Their results are in agreement with the findings of other authors [152–155] who also found that the ratio of band intensities of the bonded C=O to the free carbonyl groups decreased as the SS length decreased, i.e. when the volume fraction of the soft phase increased.

In some of our recent papers we also made evidence that polyetheric PUs phase separate to a much greater extent than the corresponding polyester-based polymers [135]. This is consistent with previous studies, that showed polyether macrodiols to give greater phase separation than polyester macrodiols [4, 14]. The reason is believed to be the availability of a $>\text{C}=\text{O}$ group on each monomer in a polyester for

possible hydrogen bonding with the >N–H groups on the HS. This lowers the free energy of mixing of HS and SS that drives phase separation, relative to those macrodiols where this is absent. The polyethers PUs are extensively hydrogen bonded which involves the N–H group as the proton donor and the urethane carbonyl, the ester carbonyl (in polyester materials) or the ether oxygen (in polyether PUs) as proton acceptor. As shown [4, 135], although nearly 100% of the N–H groups are involved in the hydrogen bonding, only 60% of the urethane carbonyls are hydrogen bonded, while the remaining N–H groups hydrogen bond with the SS. This was explained in terms of the phase intermixing of a large hard domain surface area, due to tiny domains. Srichatrupimul and Cooper [153] observed that the hydrogen bonding between the SS and HS is stronger and dissociates at higher temperatures in the interurethane hydrogen bonding.

Numerous studies of the PUs morphological features and phase segregation behaviour have been carried out by means of a variety of characterization techniques, including transmission and scanning electron microscopy (TEM) and (SEM), small angle X-ray scattering (SAXS) and atomic force microscopy (AFM), and by infrared dichroism, or thermal methods like dynamic mechanical analysis (DMA), and differential scanning calorimetry (DSC). If one could say that the variety of the techniques used to investigate the PUs phase separation suffer from emotional disorder, this would be called *phase separation anxiety*... ☺

These techniques allow visions of the microphase separation in polymers. As one can say that eye is the mirror of the soul, microphase is the mirror of the polymer structure. Remember the well known Alexander Pope's quote a few hundreds of years ago where he was asking "*why has not man a microscopic eye?*" Certainly if he had been a scientist nowadays and if he had had access to these techniques, he wouldn't have stated that man has not a microscopic eye "*for the plain reason he is not a fly*".

The first direct evidence for the formation of a two-phase structure was obtained from the SAXS studies by Bonart [156]. However detailed information could not be obtained from the single peak in their SAXS profiles without some ambiguity, as long as PUs have a disordered two-phase morphology. The two-phase microstructure was observed by Koutsky et al, by using *transmission electron microscopy (TEM)* both on polyether and on polyester PUs [157]. They found that the sizes of the hard domains varied between 30 Å to 100 Å. Later TEM works were carried out by Xu et al., Chen-Tsai et al., and Serrano et al., on the morphology of a series of TDI based PUs extended with BDO, with varying the HS fraction. The two-phase morphology was evidenced [158–160]. Yet, on the basis of the obtained evidence it still could not be assumed that complete phase separation occurred. In fact, there was evidence that appreciable hydrogen bonding exist between the HS and SS, which involved incomplete phase separation. HS domains were observed as grains of 3–10 nm dimensions by Koutsky et al [157] in solvent etched and iodine stained PUs samples by means of TEM. Finer fibrils (6 nm width) were observed by Fridman and Thomas [161]. Fibrillar structures were reported by Schneider et al. where the smallest fibrils observed were 20–30 nm in width [162]. For PUs structures of the type MDI:PBu:BG but of variable HS concentrations, Li et al. evidenced a rod-like

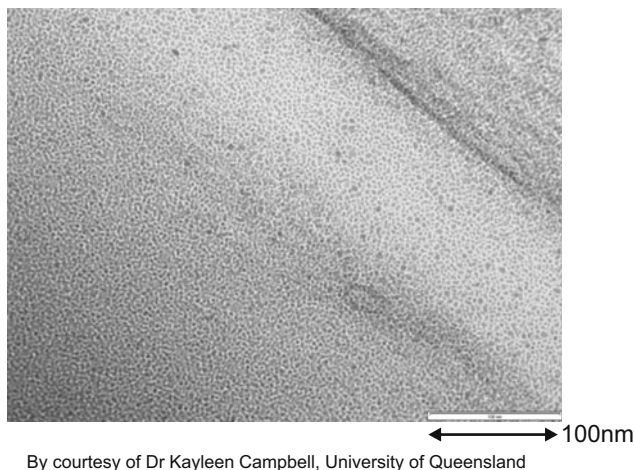


Fig. 2.3 The two-phase structure of a PU material based on MDI:PTHF:BDO. Soft domains are represented by white areas.

or lamellar structure for materials with a HS percentage of 42%–67%. At lower percentages, (<31 wt %), the HS phase was dispersed in the SS matrix in the form of short cylinders or spheroids [163, 164].

An example TEM micrograph of a MDI-BDO based PU based on PTHF ($M_w=2\,000$ g/mol), is shown in Fig. 2.3.

The use of TEM to image the nanoscale morphologies of PUs is a very useful technique that has the ability to image at high magnifications provided there is sufficient contrast between the electron density of the two phases. The electron density of one of the phases is sometimes enhanced using staining agents that make this technique dependent on the efficacy of the staining procedure. Phase separation can be detected by TEM if there is sufficient contrast between the phases. Serrano et al [165] were able to observe two phases in MDI/PBU/BDO polyurethanes even without staining, in samples with 55% and 75 wt% hard segments. Yet, TEM experiments are limited by the possibility of beam damage, and are also tedious and time-consuming due to the microtomy involved in cutting samples into few tens of nanometers thin sections. Imaging at high magnifications under TEM can also lead to misleading phase-contrast artifacts observed at a scale length of approximately 100 Å under slight defocus conditions.

Li et al used various physical methods to study the morphology of PBU based materials with variable of HS content [166]. Segmented PUs with low HS contents were found to have a morphology of dispersed short HS cylinders embedded in the matrix of the PBU based SS. An alternating HS-SS rodlike or lamellar

microdomain structure was characteristic of materials with higher HS contents. At very high HS percentages, a morphology with a dispersed SS phase was observed.

HS and SS domains can organize to form crystalline superstructures, especially in the case of solution cast samples. Spherulites with diameters from several thousands of nm up to about 20 μm were observed by *small-angle light scattering* (SALS) [167, 168], and by using *optical and electron microscopic methods* [169–171].

More recently, compositional heterogeneity has also been detected for various PUs, such as those based on poly(caprolactone) glycol PCL/PET polyesters [172] or MDI:PCL:BDO based PUs [162], by means of *gel permeation chromatography and thin layer chromatography*.

It is necessary to consider both the microphase separation of HS and SS of the same chain into different domains, and also macrophase separation of macromolecules as a whole (segregation on the molecular level) in order to explain the morphology and properties of these materials.

Small-angle X-ray scattering (SAXS) is another important tool to make evidence of SS and HS phase separation. SAXS offers several important advantages and although interpretation is less direct than are the TEM or AFM techniques, the sample preparation for SAXS avoids the potential for staining artifacts that may arise with TEM. X-rays are also less damaging to the samples than are the electron beams used in TEM, allowing measurements to be made continuously over many minutes. SAXS is used to characterize the domain structure in the size range of tens of nm. The scattering is related to morphology on the nanometer scale, but it originates from a relatively large volume (mm^3) of the material under investigation although microbeam techniques can sample smaller volumes. Therefore the results give a more statistically significant view of the morphology [173]. The X-ray are scattered by the electrons of a sample and the amplitude of the scattering radiation is given by the three-dimensional Fourier transformation of the electron density distribution. Analysis of the intensity as a function of angle reveals information regarding the morphology of the material. SAXS results for patterns of phase separated PUs show a distinct peak. This is indicative of a quasi-periodic fluctuation in electron density within these materials.

Bragg equation is used to estimate the characteristic morphological periodicity from the scattering vector corresponding to the SAXS peak position, which is related to the scattering angle and the wavelength of the X-rays. The periodicity given by the Bragg spacing corresponding to the scattering angle at peak intensity usually ranges from about 10 to 25 nm and it increases with increasing the SS molecular weight [4, 135, 173–175].

Numerous structural SAXS studies were done on PUs. For example, materials achieved with MDI-diol based HS were studied by Bonart et al [14, 15] and by Wilkes and Yusek [174]. The X-ray patterns obtained by them showed a single Bragg reflection in the diffraction pattern of the poly(MDI-BDO) hard segments at $d \approx 7.9 \text{ \AA}$, azimuthally inclined at $\sim 30^\circ$ to the meridian. In addition, an intense amorphous halo at $d \approx 4 \text{ \AA}$ was observed. Bonart assigned the Bragg reflection to planes inclined at $\sim 60^\circ$ to the fibre axis, and suggested that these planes arise from a staggering of adjacent chains so that intermolecular $\text{C=O}\cdots\text{H-N}$ hydrogen bonds

are formed between the urethane groups. This lead to the conclusion that the PU chain structure is analogous to that for the α -form of nylon 6.6.

Koberstein and Stein [136] also studied the PUs phase separation by using SAXS. The maximum in the small angle region was interpreted as the mean separation distance between the HS. The intensity profile contained information about the interfacial thickness and about the purity of the domains.

SAXS was also used by Li et al [163] to investigate the structure of a series of segmented PUs of variable HS percentage, for materials based on the couple diisocyanate-chain extender, HDI/BDO. They found that the phase structure was insensitive to the increasing HS content and thermal treatment. Structure property behaviour of the MDI/BDO based PUs was studied through the effect of composition ratio of the HS by Abouzahr et al [176]. They observed that morphological changes occur as the HS fraction is increased. The texture changed from that in which little HS domain content exists at low HS levels (15%), to that in which the polymer has an interlocking domain morphology at higher HS content (35% and 40%). Low hysteresis and high extension was obtained when isolated HS exist (25% HS). Thermal treatment of the samples lead to domain disruption and to HS-SS mixing.

In general crystalline domains are disrupted the least while the fastest recovery is displayed in samples with a non-crystalline domain texture, but this is going to be discussed to a great extent in Chapter 4 of this book.

For PU structures of a high HS content (above $\sim 30\%$), continuous HS domains could be clearly identified and traced in structural transitions [177–182]. On the other hand, the PUs of a low HS composition (less than 30%) were believed to have only discontinuous HS domains of a micellar nature [180] in the SS solvent-like matrix, especially when the sequence length of the HS is short [179]. Y.S. Sun et al [183], and L.Y. Chiang et al [184], investigated the micellar structural characteristics of segmented PUs of a low HS content and a short HS sequence length, by using the contrast variation provided by SANS and SAXS. The polyether MDI/PTMO based materials were prepared from the reaction of the chain extender BDO with diisocyanated prepolymers [184]. PUs were synthesized so that they contained 19.3 wt% hard segments. These two SAXS and SANS profiles were very similar in a wide Q range, except the sharp raising peak for SAXS in the Q region lower than 0.02 \AA^{-1} . The results indicated a general two-phase structure with low-Q sharp peak observed in the SAXS profile, which were attributed to the scattering from the partially crystalline PTMO domains of few hundreds angstroms estimated from the broad WAXS peak widths of the PTMO chains. The PTMO crystalline domains were virtually invisible to neutrons due to the very low scattering contrast [183]. The high value for the critical aggregation concentration of the HS in the PTMO matrix indicated that the HS of a short MDI sequence can dissolve in elastomer well up to $\sim 30\%$.

The increase in the HS content produces a decrease in the PUs melting enthalpy. As the melting enthalpy is related to the interactions between the polymeric chains (so-called virtual crosslinking), the trend followed by the melting enthalpy indicates that the virtual crosslinking becomes less important as the HS content increases. PUs such as those containing TDI have a high HS content and show a

melting enthalpy lower than other materials. TDI usually contains a mixture of 2,4- and 2,6-isomers and two kinds of urethane groups are possible.

Abouzahr and Wilkes also studied the effect of HS content on a series of MDI-based PUs [176]. Depending on the HS content, the properties of the elastomers were divided into four regimes. At very low HS percentages, they found that the polymer was poorly phase separated and exhibited poor elastomeric properties. At slightly higher HS contents the polymer was better phase separated, but the HS were small and isolated. This led to higher modulus, toughness and extensibility and consequently to low hysteresis. At higher HS percentages, the HS became interpenetrating and the material had a much higher modulus and hysteresis. At percentages of 50% HS and higher, the phases inverted from HS domains in a soft matrix to soft domains in a HS matrix and the polymer became brittle, high modulus plastic. Similar observations were made by us on PUs based on crystallizable HS [185].

PUs with MDI:BDO hard segments and oligomeric ethyleneoxide end-capped poly(propyleneoxide) SS containing 5-100 wt% hard blocks contents were investigated by Saiani et al [186, 187]. In their works, the PU without oligomeric diol (100% HS) exhibited one glass transition temperature and no scattering peak in the SAXS experiments, indicative of a single-phase structure. Adding just 10 wt% SS resulted in a microphase separated structure [187].

By using wide-angle X-ray diffraction (WAXD) and SAXS, Bonart et al [14] proposed a model according to which the HS were considered as extended chains.

Later, on the basis of results from SAXS and thermal analysis, Koberstein and Stein [136] and Leung and Koberstein [137] proposed a model according to which the HS domains thickness domains was controlled by the shortest HS chain insoluble in the SS phase. The HS longer than the critical length were either coiled or even folded so to be included in the HS domains. HS shorter than the critical length were dissolved in the SS phases. They also observed that the HS mobility, and the strength of the HS interaction between themselves were influenced by the *annealing temperature*. For example, in materials derived from *aromatic* diisocyanates like MDI/BDO-based segmented PUs, the HS mobility was low, and the HS interactions between them were strong, which resulted in slower phase separation after the melt was quenched to lower annealing temperatures.

Koberstein et al [180] investigated a series of thermoplastic PUs based on poly- ϵ -caprolactone SS and *aromatic* MDI:BDO based HS. To assess the hard block size on the PUs morphology, Koberstein et al. used poly- ϵ -caprolactone SS because of its miscibility with the HS. A range of block lengths showed that the compatibility level combined in polymers with smaller block lengths showed no phase segregation as indicated by SAXS measurements. The short hard block lengths were assumed to dissolve into the soft phase of such PUs systems. Increasing the block lengths, the position of the SAXS peak indicated phase separation but only of short range orders. This is consistent with a morphology with a short term order in the form of lamellar HS domains being dispersed in the SS continuous phase.

Replacing aromatic with *aliphatic* diisocyanates like 1,6-hexamethylene diisocyanate (HDI) while keeping the same structure with BDO as chain extender, resulted in HS of greater flexibility. Due to the higher HS mobility, the phase

separation rate increased owing to the relatively higher HS mobility and consequently lower PU system viscosity.

In materials obtained with aliphatic diisocyanates, the insensitivity of the hard domain length to increasing HS content has been reported for a number of HDI-BDO polyurethanes; this behaviour has been attributed to chain-folding of the lamellar morphology.

Chu et al (1992) studied the phase structure of segmented PUs as a function of the HS flexibility, by using synchrotron SAXS analysis in order to assess *the effects of thermodynamics vs. kinetics* during the phase separation [188]. Using the value of the relative invariant from the SAXS analysis and the glass transition temperature of the SS determined by DSC, they found that an increased HS content did not lead to the enhance of the phase separation. This finding does not match with the theory according to which higher HS contents lead to lower compatibility between HS and SS, which should promote phase segregation. This behaviour was explained by Chu et al., as a function of kinetics.

Other methods *associated with solid-state NMR* have been also used in numerous works to investigate the PUs phase separation behaviour [189-193]. Dumais et al., detected phase separation in NMR line broadening experiments using labeled chain extenders [191]. The two-dimensional wide-line-separation nuclear magnetic resonance spectroscopy (WISE-NMR) provides a particularly interesting alternative tool for determination of the PUs phase composition. With this experiment, a correlation has been established between chemical structure and segmental mobility as reflected in ^{13}C chemical shifts and ^1H line shapes, respectively. Segments dispersed in HS rich domains are immobilized, resulting in broad components in the ^1H spectra. The fraction of HS and SS distributed in each phase can therefore be calculated from the resolved ^{13}C spectrum. Using this technique, the degree of phase separation in piperazine-based PUs has been established [194].

The PUs microstructure can be also investigated by means of *atomic force microscopy (AFM)*. Phase images obtained via AFM, enable visual representation of the PUs microphase separated morphology. AFM records the surface topography of materials by measuring attractive or repulsive forces between the probe and the sample. Vertical deflections caused by surface variations are monitored as a raster scan drags a fine tip over the sample. A detailed description of different modes in AFM technology has been described in [195].

The use of AFM to examine the surface morphology of polymers is now well established. While different variations of AFM are available, tapping-mode AFM has gained popularity due to the lower forces involved, and because there is only intermittent contact between the sample and the tip, unlike for example in contact-mode AFM. This technique allows simultaneous detection of height and degree of phase segregation. It provides information on the variations in topography and local stiffness. '*Height*' images are obtained by storing the vertical '*z*' position of the AFM scanner-head as it scans an '*x-y*' surface, while maintaining a constant '*set point*' amplitude. Simultaneously, '*phase*' images are obtained by detecting the phase shift between the actual oscillation of a tip and its drive oscillation. In addition, since AFM images are essentially three dimensional plots of data points, this

technique also enables semi-quantitative analysis of the images by means of surface roughness and power spectral density calculations.

The AFM technique has been increasingly used as an alternative to transmission electron microscopy (TEM) for the visual interpretation of the PUs nanostructure where the surface morphology was imaged by using the tapping mode AFM. The high modulus hard domains and the low modulus soft blocks appeared as light and dark regions respectively.

The development of a PUs hard domain continuous morphology upon increasing the HS size has been investigated [196]. Using AFM, the hard domains were found to preferentially orient with their long axis along the radial direction of the spherulites. The hard domain connectivity was found to increase with increasing the percentage of HS content. For example, materials such as those based on the SS macrodiol polyethylene glycol (PEO) displayed extremely rough surfaces, limiting their resolution via AFM [176, 196]. At lower HS contents (22 wt%), the deformation mechanism involved extension of the SS. The HS were randomly dispersed in a continuous soft domain without significant aggregation which is why the alignment and break-up of the hard domain structure did not occur. At higher HS content (33 wt%), the hard domains were observed to be still randomly dispersed in a continuous soft domain, which was reflected in higher interdomain spacings. With increasing the HS content, an inter-lockong HS morphology developed, leading to the decrease of the average distance between the hard domains, which was confirmed by the SAXS studies. The development of a hard domain continuous morphology upon increasing the HS size has been observed in numerous other segmented PUs [176, 196].

PUs usually possess the microphase separated structure with interdomain spacing of 10–20 nm. But what happens if the film *thickness* is smaller than the spacing? As a rule, PUs block copolymers loose the microphase separated structure with the thickness which is smaller than the periodic structure, or forms an island structure, in which the periodic structure exists [197]. Decreasing the PUs film thickness, the size of the microphase separated domains decrease as evidenced by AFM. Decreasing the film thickness the aggregation of the HS chains becomes weaker [131].

PUs phase separation is also strongly influenced by *temperature*. The changes in the hydrogen bonding characteristics occurring in soft and hard domains are correlated with the macroscopic phase transformation as a function of temperature. Increasing the temperature above the ‘melting’ transition of the hard domains, results in a homogeneous structure accompanied by the disassociation of most of the HS–HS hydrogen bonding. If rapidly cooled (quenched), the high-temperature structure becomes “frozen”, which results in a significant number of interactions between the HS and SS. Quenching to lower temperatures retains the degree of phase mixing at the elevated temperature. If the quenched temperature is much lower than the SS glass transition temperature, the slow rate of segmental separation at low temperature prevents the reformation of the HS–HS hydrogen bonding. Raising the temperature, the low temperature structure undergoes phase separation to become a room temperature structure. In this way, direct correlation between microscopic evidence for hydrogen bonding characteristics in soft and hard domains and macroscopic

phase transformation can be obtained [149]. While the degree of microphase separation becomes weaker with increasing the polymerization temperatures, thermal treatments usually determine the increase of the degree of microphase separation [198, 199]. When the PUs are annealed at certain temperatures, the HS domains with melting points above the annealing temperature are progressed.

2.2 Phase separation kinetics

Every process which is not forbidden must occur. (totalitarian principle)

Remember the totalitarian principle according to which “*every process which is not forbidden must occur*”? Not only the characterization of the PUs phase separated structure is important, but, from the perspective of PUs fundamental point of view, the mechanism associated with the phase separation is also extremely important and equally interesting. Occurrences in the phase separation process are strongly affected by the variety of parameters in operation.

Phase separation kinetics for PUs block copolymers has been extensively studied. Various techniques have been applied to study the aspects of PUs phase separation kinetic behaviour. For example, scattering techniques, mainly SAXS can give the average size of the hard domains evolving from a homogeneous single phase. By monitoring mechanical properties as a function of phase separation time, the phase separation kinetics can also be deduced, but the direct relationship between the macroscopic mechanical properties and the degree of phase separation is generally hard to establish.

The rate and degree of phase separation depends on structural parameters such as interaction parameter between two phases, presence of hydrogen bonding and crystallization of one or both phases, segment size and segment size distribution, and also experimental conditions, i.e. annealing and storing temperature and time) [4]. The rate of phase separation depends on the regime of cooling, or isothermal temperature if the process is studied isothermally. In general the experiments consist of heating the PUs sample at high temperature (annealing) and then quenching to a storage temperature, at different time intervals. On quenching, HS ordering needs pulling of the SS ends, while stretched SS retractive forces act during reheating of the sample, which may cause HS disruption. This leads to partial mixing of phases, at elevated temperatures, above the glass transition temperature of the HS. Heating above the melting point of the hard phase causes complete mixing with SS [4]. At high temperatures part of short HS are soluble in the soft phase. Decreasing temperature, shorter and shorter segments become excluded.

A series spectroscopic analysis of the phase separation kinetics in model PUs was made by Lee et al [200]. Isothermal phase separation kinetics was studied by raising the PUs sample temperature quickly to the phase separation temperature and measure the changes in the infrared spectrum at constant temperature. They assigned spectroscopic features characteristic of urethane linkages dispersed in the

SS as compared to interurethane hydrogen bonding confined to the HS domains. With a specially designed sample cell [200], they trapped a phase-mixed structure at a temperature 60°C below the glass transition temperature of the SS. When the quenched PU sample was brought up to a higher temperature, the increase of one spectroscopic component and the corresponding decrease of the other provided a direct measurement of phase-separation kinetics.

The results of the study clearly indicated that the phase separation process involves a gradual transfer of the HS dissolved in the soft matrix into the hard domain. As shown [200], frequency and intensity differences at different temperatures for both the hydrogen bonded and free C=O vibrations can be significant and difficult to define. However the measurement of the relative intensity of the two components at constant temperature removes this difficulty.

2.3 Structural studies on polyurethane elastomers with crystallizable hard segments

Crystallization is the action of the mind that discovers fresh perfections ... at every turn of events. (Stendhal)

“Crystallization” is a concept developed in 1822 by the French writer Stendhal, to describe mental metamorphosis. In the summer of 1818 Stendhal went to the salt mines of Hallein near Salzburg with his friend Madame Gherardi, where they discovered the phenomenon of salt “crystallization”. He defined the term “crystallization” and used it as a metaphor for human relationships. *Remember Stendhal’s* classic (1882) “De l’Amour” where he explains crystallization as a natural “mental process” drawing from proofs of the perfection. Imagine a tree branch covered with crystal deposits left in Salzburg’s salt mines for a few months.

The notion of “crystallization” was pivotal for Stendhal who extended this metaphor into his theories on art and on literature: the process of making and perfecting art and the evocative power of the artist. He defined them as “crystallization processes”.

Obviously the author of “Le Rouge et le Noir” wouldn’t have imagined that the “crystallization” concept defined by him, will be extended to describe things like polymers. Moreover, in terms of crystallization, the morphology of polymers is even much more complicated—although I am sure artists or writers would dislike this.☺ But here, while writing this, I feel on a safe territory, far from people of art, so I can dare to make such an assertion.

It is axiomatic that an individual polymer molecule which possess a high degree of chemical and structural regularity among its chain elements is capable to undergo crystallization. For a polymer with a high regular ordered, structure, conditions must be found that are kinetically favourable for crystallization.

The understanding of the structure and properties of semi-crystalline polymers involves numerous variable techniques and theoretical approaches. Essentially, all

Fig. 2.4 Extended linear
“anti” DBDI position

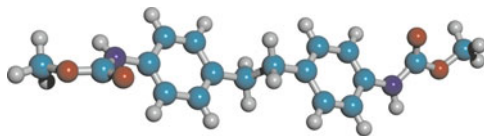


Fig. 2.5 Contorted “syn”
DBDI position

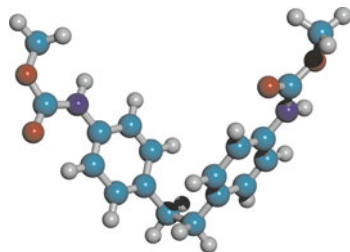
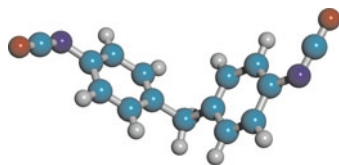


Fig. 2.6 Conventional rigid
4,4-diphenylmethane di-
isocyanate (MDI) non-
crystallizing



properties are controlled by morphology, which in turn is determined by the crystallization mechanisms. From the thermodynamic point of view, the nature of a crystallization process is governed by both thermodynamic and kinetic factors, which can make it highly variable and difficult to control.

PU morphology is very complicated not only because of the two-phase structure, but also because of other physical phenomena such as *crystallization* and hydrogen bonding in such systems. The crystallinity of phases and the size of domains along with the molecular composition, control the PU morphology and macroscopic properties. Crystallization of the HS is an important determinant of the extent of phase separation, and the development of crystallinity is dependent on the hydrogen bonding and other interactions between the chains in the hard domains [201].

Crystallinity has been observed in the soft phase when the macrodiol chain is long enough, and it is also sometimes present in the hard phase. The latter is usually limited to only a few percent for most HS structures when solidified from the melt, but there is one particular diisocyanate, *4,4'-dibenzyl diisocyanate (DBDI)* that, in the presence of suitable chain extender, gives rise to significant degrees of crystallinity [60, 61, 135], and this is included and detailed in the present book.

As reported by ourselves [60, 61, 135] and by Lyman and Gowerr [58, 202], the MDI molecule introduces the rigid $-\text{Ph}-\text{CH}_2-\text{Ph}-$ moiety in the elastomeric PU hard segments. In contrast when using DBDI, the specific $-\text{Ph}-\text{CH}_2-\text{CH}_2-\text{Ph}-$ moiety introduces a variable geometry into the hard segments due to the possibility of internal rotation of this isocyanate around the $-\text{CH}_2-\text{CH}_2-$ ethylene bridge.

This leads to the appearance of both “anti” and “syn” rotational conformations, which coexist in the DBDI based PU macromolecules, (Fig. 2.4–2.6). As a result, in this latter case the PU macromolecules can adopt a more compact packing which enhances significantly the ability to order in crystalline structures involving predominantly the “anti” form [60]. Shown in Fig. 2.4 and 2.5 are the extended linear “anti” and contorted “syn” DBDI positions as compared to the conventional rigid 4,4-diphenylmethane diisocyanate (MDI) non-crystallizing (Fig. 2.6).

The rotational isomerism of the dibenzyl biaromatic (DBDI) systems allows multiple spatial arrangements, with different reciprocal influences of the functional groups situated in the two rings. As shown, the angle between the plane and the $-\text{CH}_2-\text{CH}_2-$ linkage is 70.5° . As earlier shown in this book, by studying the reactivity of DBDI and comparing it with other conventional diisocyanates, we concluded that the reactivity of DBDI was very similar to that of the conventional rigid diisocyanate MDI [45].

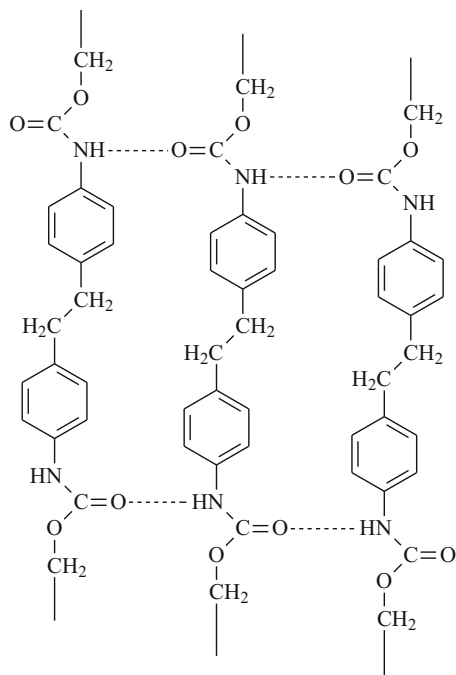
The PUs with DBDI based HS investigated by Caraculacu et al [59] showed a fiber repeat distance which is that expected for a fully extended chain. In this conformation, chains readily pack to form fully hydrogen-bonded sheets. The X-ray diffraction spectrum showed a periodicity of $19.7 \pm 0.2 \text{ \AA}$ and was similar to that of the triclinic form of nylon 66, nylon 6 and nylon 8 [59]. This was in contrast with the analogous materials based on the conventional rigid diisocyanates like MDI, where the extended chain conformation has the appearance of a large zig-zag structure where, although chains with this conformation can be readily packed together, only one half of the potential hydrogen bonds are formed [59]. In the case of the materials with MDI, X-ray determination showed a periodicity of $15.7 \pm 0.1 \text{ \AA}$ with qualitatively similar arrangement but belonging to the hexagonal lattice crystalline system [59]. As previously shown by us, in polymers with MDI, the HS are associated but not so ordered as they are in the materials with DBDI where HS are both ordered and associated, which determines a crystalline PU structure [59, 60].

A conformational mobility of the diisocyanate like DBDI (Fig. 2.7) may cause an unusually wide range of mechanical, physical and chemical properties, associated with the possibility of pronounced phase separation into a domain-matrix morphology, and with a higher tendency to crystallization and self-association by hydrogen bonding [61, 127]. Hard domains having a higher flow stress in the presence of the diisocyanate DBDI, have been associated with increased hydrogen bonding which was enhanced in numerous cases by HS crystallinity [61]. The primary effect of employing flexible HS in the PUs synthesis, was shown to be a closer self-association of HS by hydrogen bonding.

Shown in Fig. 2.8 (a) and (b) are example microphotos of the two-phase structure for two analogous materials based on PTHF of molar mass 2 000 g/mol and chain extended with BDO. They differ only in the type of diisocyanate, the rigid MDI or DBDI displaying a variable geometry. Transmission optical microscopy standard method was used to investigate the microstructures.

Both images reveal clear heterogeneity of the samples. This is consistent with previous observations made by ourselves and by others on polyether macrodiols based PUs to give greater phase separation than polyester macrodiols [4, 14],

Fig. 2.7 2-D network of hydrogen bonds in a DBDI based material



regardless the type of the diisocyanate used in the PU synthesis. Moreover, the inclusions ($2\text{ }\mu\text{m}$ diameter or less) observed in the DBDI based structure were associating with a higher tendency to HS crystallize characteristic for materials based on the couples DBDI-EG or DBDI-BDO [61].

In the DBDI based polymers there was a clear indication from data that the physical origin of the flow stress must be relative displacement of the hydrogen-bonded HS [61, 135, 175]. In deformed PUs, the anisotropy of the structures relative to the strain direction was clearly visible in the 2D images (Fig. 2.9). Samples were

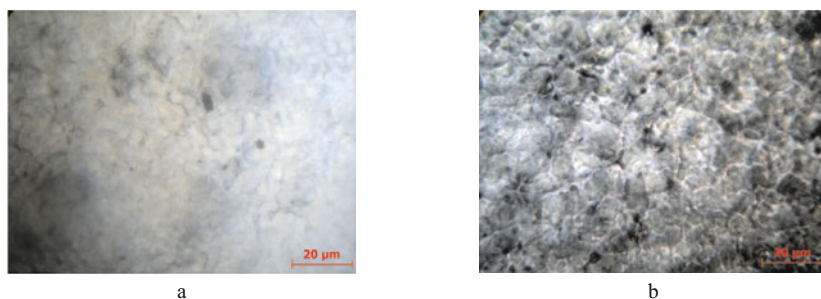


Fig. 2.8 Example two-phase structures: (a) MDI:BDO:PTHF; (b) DBDI:BDO:PTHF at 1 000 μm magnification

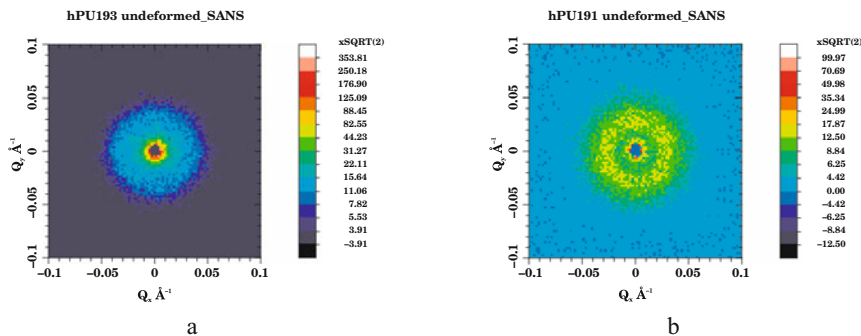


Fig. 2.9 SANS patterns from two bulk PU elastomers; they differ only in the type of diisocyanate, the flexible DBDI and rigid MDI: (a) DBDI:BDO:PTHF; (b) MDI:BDO:PTHF; by courtesy of Dr. D. Bucknall, Virginia Tech University.

strained to up to 300% levels of extension. Depending on the type of diisocyanate (crystallizing or not), they showed various degrees of anisotropy, with the highest values corresponding to the PTHF/DBDI based materials. The macroscopic deformation was present in the molecular levels that were probed with neutrons.

There were tendencies to phase separation, with a characteristic length of ca 20 nm, and, when DBDI was employed with BG or EG, to crystallization of the hard phase through its effect of increasing the flow stress.

In our previous beam time (RB510315) we observed a strong scattering peak at low Q in the various PUs (see Fig. 2.10) which is consistent with the microphase separation in block copolymers predicted by Leibler [203]. The phase domain dimensions varied between 10-20 nm, depending on the PUs specific composition. After straining to 300% (Fig. 2.10) the morphology is clearly disrupted with a reduction or in some PUs a total loss of domain structure.

The AFM method was also used by ourselves to examine and compare DBDI with MDI based films surfaces and to measure their surface topography. Topographical and phase contrast AFM images were taken from different zones of the materials. The replacement of DBDI with MDI determined morphological variations and a decrease of the average height texture parameter, both for the molten and for freeze fracture surfaces. The separation between crystalline and amorphous phases was better observed in the AFM phase contrast images. The crystalline domains were observed to have higher hardness while the amorphous domains have higher elasticity. The separation between crystalline and amorphous phases was more pronounced in the DBDI polymer. Example topographical and phase contrast AFM images for freeze fracture surfaces are shown in Fig. 2.11 for the same two materials (analogous structures) as in Fig. 2.8 and 2.9. They differ only in the type of diisocyanate, the model rigid MDI or the flexible DBDI.

The SEM investigation made by us clearly revealed the strong influence of the variable geometry of the diisocyanate DBDI on the formation of hard domains with a pronounced crystallinity, especially when EG or BDO were employed as chain

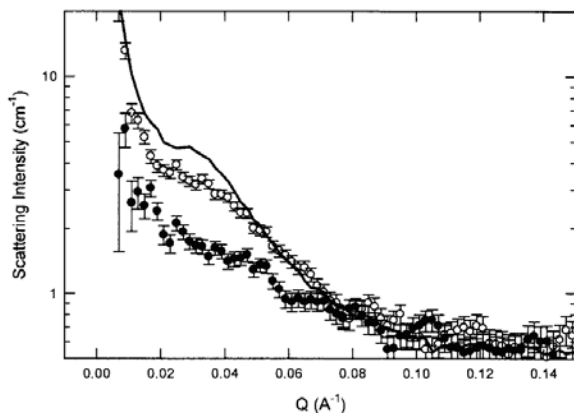


Fig. 2.10 SANS scattering from a fully hydrogenous PU before (solid line) and after straining to 300%, with data in the parallel (open circles) and perpendicular (solid circles) to the draw direction.

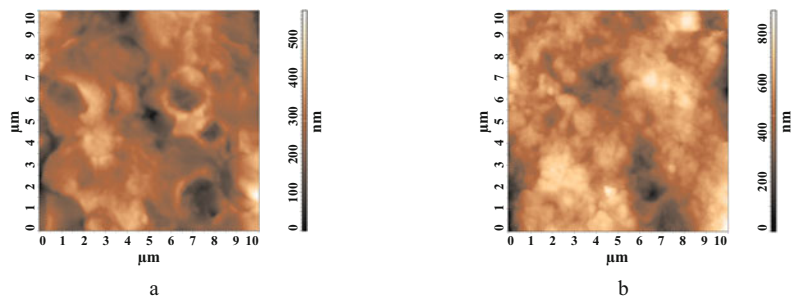


Fig. 2.11 Topographical and phase contrast AFM images for freeze fracture surfaces for two analogous materials; they differ only in the type of diisocyanate. (a) (DBDI:BDO:PTHF); (b) MDI:BDO:PTHF. Courtesy by Mrs. I. Stoica, Institute of Macromolecular Chemistry, Petru Poni, Iasi, Romania

extenders. Shown in Fig. 2.12 and 2.13 are the SEM pictures of two PUs with similar structures, where only the type of isocyanate differs: MDI non-crystallizing, DBDI crystallizing. With DBDI the polymer matrix becomes more mobile and allows the chain extender-diisocyanate segments to move and crystallize in self-associations [204]. Investigation of PUs by means of SEM revealed the fact that the nature of the hard phase and the degree of phase separation in PUs can be controlled via the chemical structure.

The materials displayed a relatively coarse structure on 10 μm scale but which varied between the polymers. Fig. 2.12 displays the features of a DBDI based original sheet. At 0.1 mm magnification the arrow points to a particularly prominent area of the banding which is typical of this specimen. The most prominent feature is what is referred to as the *coarse structure* of about 10 μm in scale: this is due

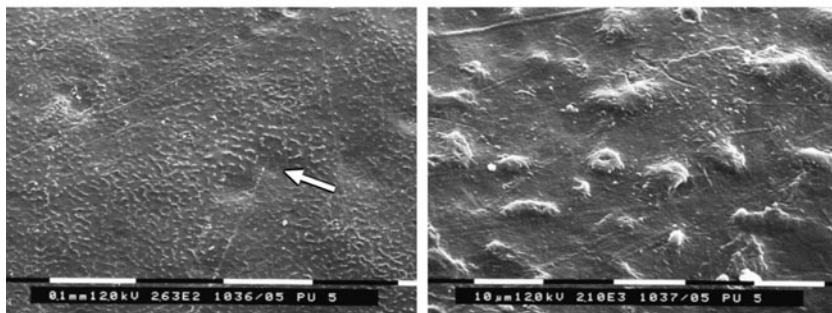


Fig. 2.12 SEM of a PU based on DBDI (original sheet) at two magnifications [204].

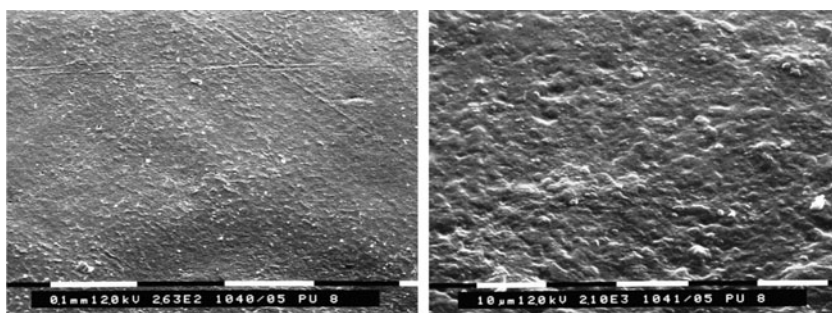


Fig. 2.13 SEM of a PU based on MDI (original sheet) at two magnifications [204].

to large extent of PU phases separation in the dibenzyl-based material. There are only the faintest hints of a texture on this scale in the equivalent material with MDI. This banding is made up of phase-segregated lumpy regions, which are either finer or not present at all in the material with MDI. Fig. 2.13 displays the features of the analogous MDI based PU original sheet. The banding also appears, but much less pronounced. PU with DBDI which displays X-ray crystallinity [60, 127] tends to give a rougher surface morphology than PU based on MDI.

The most prominent feature is what is referred to as the coarse structure which is due to large extent of phases separation in the polymers derived from DBDI. As previously shown, the dibenzyl based polymers did not retract after rupture [204]. After step stretching of the materials, the presence of the dibenzyl structures gave a much rougher surface morphology than that observed in the MDI based polymers [204].

Several chemical etching techniques were tried on these materials. In Fig. 2.14, etched surfaces of MDI and DBDI based materials are shown.

In the material based on MDI (Fig. 2.14(a)), the relatively resistant material is in majority, with non-resistant pockets being consumed by the etchant. As observed elsewhere [60], such pockets represent materials precipitated during polymerization.

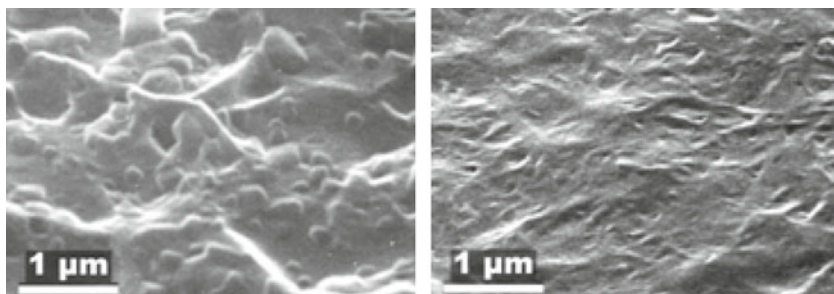


Fig. 2.14 SEM of etched PU specimens: (a) MDI; (b) DBDI [204].

In the materials with DBDI (Fig. 2.14(b)) the overall etched texture is much flatter. The regions of chemical segregation are more or less equally attacked. The material with DBDI does not show the precipitated crystals. A more detailed SEM description on the morphology of MDI and DBDI based PUs and mixtures of them, is made in section 2.3.2.2. where the materials are characterized and compared from two perspectives: (a) effect of the SS macrodiol nature (polyester or polyether); (b) effect of type, and number of diisocyanates (crystallizing or not) and their order of introduction in the reaction synthesis.

2.3.1 Structural studies on polyurethane elastomers obtained with single diisocyanates

The degree of phase segregation between HS and SS depends both on the degree of interaction between the HS to each other and towards the SS and on the mobility of the polyurethane chains. Hard domains having a higher flow stress in the presence of the diisocyanate DBDI, have been associated with increased hydrogen bonding which was enhanced in numerous cases by HS crystallinity [60, 61, 135]. The primary effect of employing flexible HS in the PUs synthesis, was shown to be a closer self-association of hard segments by hydrogen bonding. In such polymers there is a clear indication from data that the physical origin of the flow stress must be relative displacement of the hydrogen-bonded HS.

A systematic study of PUs with HS of variable crystallinity was made by us [60, 61, 127, 135]. Two diisocyanates were considered: the frequently employed MDI, and its close relation DBDI, that is of special interest because of its tendency to crystallize on cooling from the melt in the presence of some chain extenders [135]. The family of model PUs was synthesized for this work in the authors' Romanian laboratory. They were all three-component systems combined in stoichiometric proportions, and consisting of: (1) a diisocyanate—either MDI or DBDI; (2) a SS macrodiol—PEA, PTHF, or PBA; and (3) a small molecule diol as chain

extender—anhydrous EG, DEG, or BDO. The macrodiols were all of molar mass 2000 ± 50 g/mol.

The three components were always mixed in the molar proportions hard segment:macrodiol:chain extender = 4:1:3, giving hard segment mass fractions in the region of 40%, and isocyanic index $I = 100$ which means that they are truly thermoplastic. They do not have the potential for further reaction with ambient humidity to produce chain lengthening and allophanate cross-linking, seen in similar polymers but with excess isocyanate groups (e.g. $I = 110$). Synthesis was carried out by the prepolymer route described previously by Prisacariu et al [135]. Information on the nanometre-scale physical structures of the materials was gained by X-ray scattering, using synchrotron radiation at the UK Daresbury Laboratory. Wide-angle X-ray scattering (WAXS) studies were carried out using Station 16.2 SMX, with X-ray wavelength 82 pm. The 2D patterns were radially averaged to produce 1D intensity profiles, as illustrated in Fig. 2.15. In some of the materials, predominantly some of those based on DBDI, sharp peaks were observed in the WAXS intensity versus 2θ scans, indicating some crystallization of the hard segments [135]. There was no indication of crystallinity arising from the soft segments in these materials. The scattering intensity was separated into amorphous halo (I_a) and crystal diffraction (I_c) components by fitting Gaussian peaks to those crystal diffraction peaks visible, following the procedure used in a previous paper [135], and a degree of crystallinity χ was determined from the ratio of the integrated intensities:

$$\chi = \frac{\int I_c d\theta}{\int (I_a + I_c) d\theta} \quad (2.1)$$

Values of χ are included in Table 2.1.

Small-angle X-ray scattering (SAXS) studies were carried out using Daresbury Station 16.1 with the RAPID 2-dimensional detector, with X-ray wavelength $\lambda = 141$ pm and a camera length of 4 m. Scattering intensities were radially averaged, to obtain 1-D patterns of intensity versus $q = \left(\frac{4\pi}{\lambda}\right) \sin \theta$. Three features are of particular interest.

Firstly, wide variations were observed in the scattering intensity for different materials, indicating differing degrees of phase separation. This was quantified as follows, following Saiani et al [187]. For each scattering pattern, the measured intensity (in arbitrary units) was normalized for specimen thickness and incident beam intensity. Then the high q tail of the curve of normalized intensity $I_n(q)$ was fitted to Porod's Law for scattering by a two-phase system with sharp phase boundaries $I_n = \frac{K}{q^4} + I_b$. Excellent agreement was found in all cases except PU₁. For the other polymers the mean R^2 for fitting to Porod's Law was 0.996. These fits provided the background intensity I_b (assumed independent of q) and Porod constant K . The corrected intensity $I = I_n - I_b$ was then employed in determining the relative scattering invariant Q from the relation

Table 2.1 Chemical and physical structures of the PUs studied in this work. Q is the relative SAXS scattering invariant obtained from the intensity distribution, d is the dominant long period obtained from q^* the position of the peak SAXS intensity, A/V is the particle surface-to-volume ratio obtained from SAXS, and χ is the degree of crystallinity as determined from WAXS [135].

Material	DI	MD	CE	Hard segment volume fraction ϕ_H	Q	d Nm	A/V Nm^{-1}	χ
PU ₁	MDI	PEA	EG	0.356	0.82	-	-	0.036
PU ₂	MDI	PEA	DEG	0.380	2.46	18.7	0.722	0
PU ₃	MDI	PEA	BG	0.372	2.30	14.1	0.816	0
PU ₄	DBDI	PEA	EG	0.363	5.69	16.0	0.822	0.165
PU ₅	DBDI	PEA	DEG	0.387	2.32	22.0	0.721	0
PU ₆	DBDI	PEA	BG	0.378	2.47	16.8	0.659	0.104
PU ₇	MDI	PTHF	EG	0.326	28.69	21.0	0.441	0.012
PU ₈	MDI	PTHF	DEG	0.350	11.40	22.8	0.572	0
PU ₉	DBDI	PTHF	EG	0.333	34.35	18.7	0.753	0.158
PU ₁₀	DBDI	PTHF	DEG	0.356	22.91	20.1	0.519	0
PU ₁₁	MDI	PBA	EG	0.323	5.64	18.7	0.586	0
PU ₁₂	MDI	PBA	BG	0.338	5.47	16.8	0.835	0.027
PU ₁₃	DBDI	PBA	DEG	0.344	4.96	-	0.536	0
PU ₁₄	DBDI	PBA	BG	0.354	6.28	16.2	0.556	0.183

$$Q = \int_0^{\infty} q^2 I(q) dq \quad (2.2)$$

where the upper end of the range of integration, beyond where data were available, was obtained with the extrapolation $I = \frac{K}{q^4}$.

Secondly, all but two of the scattering patterns obtained showed a distinct peak, at a position q^* in the region of 0.3 nm^{-1} . In these cases, a “long period” d was calculated from $d = \frac{2\pi}{q^*}$, representing a dominant repeat distance of the two-phase structure causing the scattering [135].

Finally, the availability of both parameters K and Q enabled another structural measure to be estimated: the particle surface area-to-volume ratio A/V . It was obtained as follows [205]:

$$A/V = \frac{\pi K}{Q} (1 - \phi_h) \quad (2.3)$$

where ϕ_h is the volume fraction of particles: hard diisocyanate-rich domains in the present materials. Note that ϕ_h could only be approximated, since the exact composition and densities of particles and matrix are unknown. In applying equation (2.2), it was approximated by its theoretical limit in the case of complete phase segregation, i.e. the HS volume fraction ϕ_H , calculated from the HS mass fraction, the density of the HS (taken to be 1.29 g/ml for DBDI and 1.27 g/ml for MDI [187]),

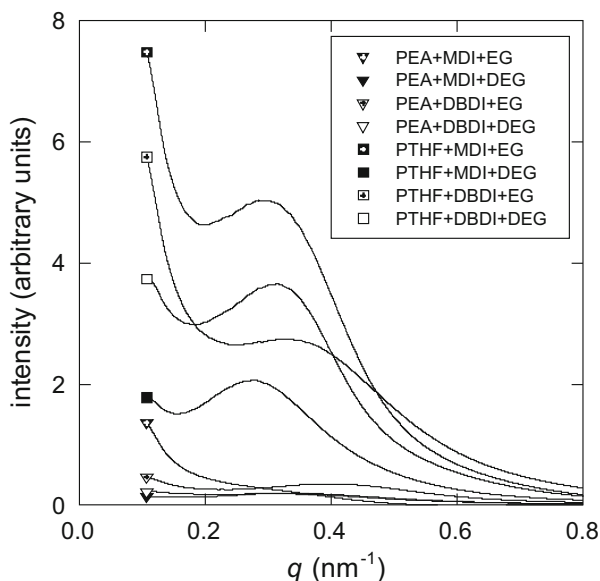


Fig. 2.15 Example 1-D SAXS patterns normalized and baseline-corrected as described in the text, for eight of the materials listed in Table 2.1, with compositions shown [135].

and the density of the SS (taken as 1.18 g/ml for PEA, 1.04 g/ml for PTHF and 1.02 g/ml for PBA). Values of ϕ_H , Q , d and A/V are included in Table 2.1.

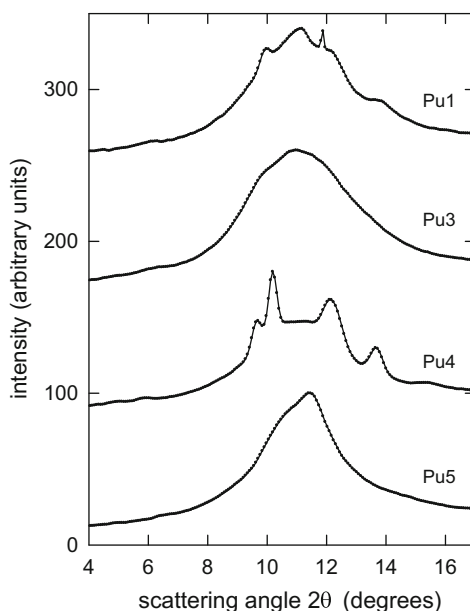
Fig. 2.15 shows SAXS patterns for eight of the materials, providing evidence of phase separation in the present series of materials. But Fig. 2.15 also reveals that the SAXS intensity, indicating the degree of phase separation, varies greatly between the materials. In particular, it is clearly visible that the polymers with strongest scattering are those with PTHF as macrodiol. This result is quantified in Table 2.1, where the values of relative scattering invariant Q provide numerical measures of the relative degree of phase separation, since it depends on the hard phase volume fraction ϕ_h and the difference in electron density (ρ_e) in hard (h) and soft (s) phases as follows [135, 187]:

$$Q \propto \phi_h(1 - \phi_h)(\rho_{e,h} - \rho_{e,s})^2 \quad (2.4)$$

In the arbitrary units of Q in Table 2.1, the PTHF-based polymers PU₇, PU₈, PU₉ and PU₁₀ have Q in the range 11-34, while all the other polymers have smaller values in the range 0.8-6 [135].

The observation that PTHF-based PUs phase-separate to a greater extent than the corresponding PEA and PBA-based polymers is consistent with previous studies of polyurethanes, that showed polyether macrodiols to give greater phase separation than polyester macrodiols [4, 135]. The reason is believed to be the availability of a $>C=O$ group on each monomer in a polyester for possible hydrogen bonding with the $>N-H$ groups on the hard segments. This lowers the free energy of mixing of

Fig. 2.16 Example 1-D WAXS patterns for four representative materials: all are based on PEA as macrodiol but differ in diisocyanate and chain extender. PU₁ (MDI+EG) is slightly crystalline (4%), PU₃ (MDI+BG) is amorphous, PU₄ (DBDI+EG) is significantly crystalline (17%), PU₅ (DBDI+DEG) is amorphous. Consecutive patterns have been shifted vertically 80 units for clarity [135].



hard and soft segments that drives phase separation, relative to those macrodiols where this is absent, such as the polyethers.

Fig. 2.15 also shows that the SAXS patterns of most polymers had pronounced peaks in intensity, indicating a dominant repeat distance for the 2-phase structure. As quantified by the long period d , this varied from 14 to 23 nm. Such values for d and the values of hard domain area-to-volume ratio A/V listed in Table 2.1, emphasise the small sizes of the domains. An important consequence for the mechanical properties of the materials is that a large fraction of the hard segments must therefore reside at the surfaces of the domains. This fraction may be quantified in terms of $\nu^{1/3}$ where ν is the volume of one hard segment monomer: in the present materials it varies between ca 32% (PU₇) to 62% (PU₁₂). Finally, another notable implication is that molecular mobility within the soft matrix must suffer significant constraint from the excluded volume of the hard domains. An approximate measure of the average width of the gap between domains may be obtained from $(V/A) \frac{1-\phi_H}{\phi_H}$. The values in Table 2.1 indicate this quantity varies between 2.1 nm (PU₃) and 4.6 nm (PU₁₄) [135]. In addition, mobility in the soft phase must be reduced by their molecular connection to the relatively immobile segments of the hard domains.

WAXS patterns gave evidence of hard phase crystallinity in some of the materials [135]. Fig. 2.16 illustrates the range of types of pattern obtained: DBDI-based polymers with intense sharp peaks indicating significant crystallinity (PU₄), DBDI-based polymers with no sharp peaks indicating no crystallinity (PU₅), MDI-based polymers with low intensity sharp peaks indicating very slight crystallinity (PU₁), and MDI-based polymers showing only an amorphous halo (PU₃).

Table 2.1 includes the degree of hard segment crystallinity χ for all the materials. It is notable that all the MDI-based polymers show no, or only slight, crystallinity (maximum 4%). The only polymers to have more significant crystallinity are those based on DBDI. This is consistent with previous reports of comparisons between melt-processed polyurethanes based on these two diisocyanates [60, 202]. But the presence of DBDI does not always lead to crystallinity: it depends on the choice of chain extender. In Table 2.1, the DBDI-based polymers with DEG as chain extender can be seen to have no detectable crystallinity, whereas those with EG and BG have degrees of crystallinity up to 18%.

The relative ease of crystallisation in DBDI as compared to MDI is readily explained in terms of greater flexibility of the DBDI molecule, arising from its $-(CH_2)_2-$ bridge between the phenyl rings, compared to only $-CH_2-$ in MDI [60, 202]. Thus DBDI hard segments can adopt a linear conformation facilitating packing and inter-chain hydrogen bonding. MDI hard segments, however, are intrinsically kinked in shape, reducing conformational mobility and thereby hindering close packing and achievement of hydrogen bonding [60, 202]. Conversely, when DEG is used as chain extender with DBDI, the central $-O-$ atom introduces kinks into the DBDI hard segment and disrupts the chain packing that could otherwise be achieved [61].

Fig. 2.17 shows example WAXS and SAXS correlated patterns for the PEA, PBA and PTHF-based materials labeled in Table 2.1, providing evidence of phase separation in the present series of materials. The polymers with strongest scattering are those with PTHF as macrodiol, irrespective of the type of diisocyanate (crystallizing or not). The crystallinity index (χ) revealed by WAXS experiments, was higher for PUs with DBDI, extended with EG or BG at lower SAXS peak areas. These two chain extenders lead to distinct diffraction peaks. Inelasticity was greater for DBDI hard segments than for MDI [61, 175]. *Irrespective of the choice of diisocyanate (MDI or DBDI), all materials with PTHF showed much higher intensity in SAXS.* Such PUs have fewer H bonding: only 40% of the carbonyl in polyether urethanes are hydrogen bonded than polyester urethanes (PEA, PBA) with same HS content.

Materials derived from DBDI and PTHF showed both crystallinity and high phase segregation. This was in contrast with the analogous structures but achieved with MDI where the crystallinity was absent, but the materials also showed high phase segregation. There was evidence of the appearance of more or less complete phase separation associated with the formation of discrete crystalline hard domains.

The PUs excellent properties of originate mainly from their special tendency to form discrete regions in which the HS made up by diisocyanate and extender tend to self associate in separate microdomains. Sometimes these associations are ordered to such an extent that they can be evidenced by their characteristic X-ray diffraction.

A good way for us to study this process was to take into account *homopolyurethanes* as *simple model substances*, which reproduced the structure of the HS from the different complex PUs.

Simple model homopolyurethanes $[EG-MDI]_n$ or $[EG-DBDI]_n$, were achieved by us. The X-ray diffraction patterns showed a significant tendency to crystallize for the dibenzyl based PUs. Fig. 2.18 shows example WAXS diffractograms for a DBDI

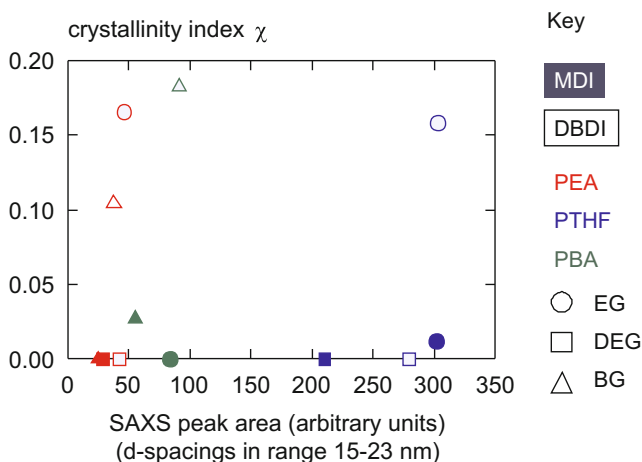


Fig. 2.17 X-ray characterization of the nano-scale structure for example PUs, plotted as crystallinity index (χ) versus SAXS peak areas; filled symbols — data for MDI-based polymers; open symbols — data for DBDI-based polymers [175]

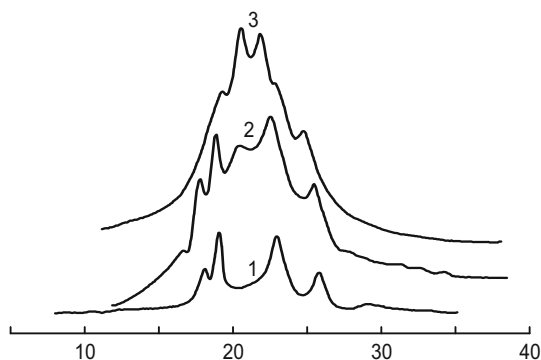


Fig. 2.18 Wide-angle X-ray scattering from: (1) homopolymer EG-DBDI; (2) – PU (DBDI:PEA:EG) with molar ratio EG/PEA = 3; (3) – PU (DBDI:PEA:EG) with molar ratio EG/PEA = 2.64 (PU₁) [206].

material obtained with EG and PEA, with the molar ratios EG/PEA = 3 (curve 2), and EG/PEA = 2.64 respectively (curve 3) [206]. Curve 1 is for the corresponding homopolyurethane [EG-DBDI] based on HS only.

For the DBDI-based material and its corresponding homopolyurethane [EG-DBDI]_n (curve 2) the crystallization did not disappear with the inclusion of the HS in the block copolyurethane elastomeric matrix, indicating the appearance of more or less phase separations associated with the formation of crystalline hard domains. As seen, curve (2) for the material with molar ratio EG/PEA = 3, was very similar with curve (1) corresponding to the homopolymer, and proportional to HS

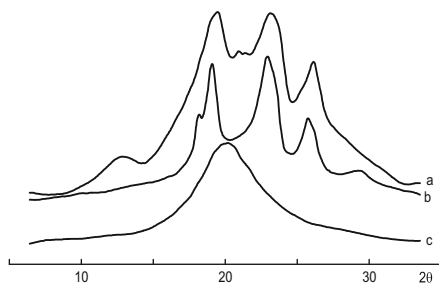


Fig. 2.19 WAXS of polyurethanes containing only hard segments: (a) [BDO–DBDI]_n; (b) [EG–DBDI]_n; (c) [EG–MDI]_n [60]

content. Reducing the number of HS by lowering of molar ratio from 3 to 2.64 determined significant changes in the shapes of the diffractograms [206]. There appeared crystalline structures of other types, within which the SS were involved also.

Fig. 2.19 displays some other typical WAXS curves. As shown [60] [EG–DBDI]_n represents a polymer with a high tendency of crystallization (Fig. 2.19 (b)) both in terms of quantity of crystalline material and the definition by the X-ray reflections. This behaviour is paralleled by the self-separation of crystalline polymer from its solution with time [69]. The [EG–MDI]_n (Fig. 2.19 (c)) shows only a single broad peak, rather narrower than might be expected for an amorphous halo, suggesting a rather loose association of molecular chains. This material does not crystallize from solution [60].

This capacity for crystallization is characteristic not only for the [EG–DBDI]_n structure, but also for similar DBDI based materials produced by changing the glycol as for example in the case of a [BDO–DBDI]_n structure Fig. 2.19 (a). As shown, an extender with an even number of methylene units should allow the diisocyanate molecule to assume an almost linear “anti” conformation, so these materials should exhibit an ‘odd-even’ variation in their ability to crystallize as observed in similar cases [60].

The WAXS patterns showed that the crystallizability of DBDI based material largely remains even after the inclusion of the SS; this indicated the appearance of more or less complete phase separation associated with the formation of discrete crystalline hard domains. The presence of these structures induced a special mechanical behaviour in these elastomers as you will see in Chapter 4. Due to the disordered orientation of these domains in the polyether matrix the materials appear initially isotropic on the macroscale but when subjecting the polymer to stretching, some microdomains tend to orient in parallel, maintaining to some extent the so obtained anisotropy even after removing the stress. As a result some enhanced residual elongation was evident and the chain orientation was substantially confirmed by using a polarizing optical microscope. Supplementary studies on this subject were performed employing IR dichroism [60].

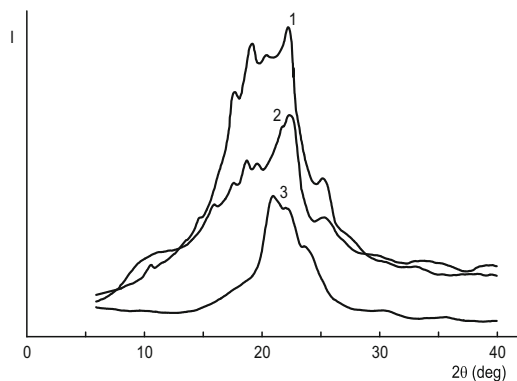


Fig. 2.20 Wide-angle X-ray diffraction from a PU of type D (DBDI-PEA-BDO, $I = 110$): (1) PU sheet cast directly from synthesis; (2) PU film obtained by evaporation from 10% solution in DMF; (3) PU film obtained by evaporation, then stretched to 300% elongation, and then released for 24 hours (residual elongation 175%); intensity scan perpendicular to the direction of elongation [60].

It is also noteworthy, however, that *the sample preparation technique also influences PU crystallization*, as shown for the case of a dibenzyl PU (DBDI:PEA:BDO) in Fig. 2.20. The crystallinity of the materials with DBDI is more pronounced when the polymer is obtained as a sheet cast directly as a melt following synthesis (Fig. 2.20, curve 1) than when the same PU has been obtained by evaporation from 10% solution of DMF (Fig. 2.20, curve 2). The crystallinity also changes completely if the solution-cast PU film is stretched to 300% elongation and released (Fig. 2.20, curve 3).

2.3.2 Structural studies on polyurethane elastomers obtained with mixtures of diisocyanates

As shown above one of the convenient means to reduce the DBDI based PUs crystallinity was to use the flexible chain extender diethylene glycol (DEG), which inhibits crystallization. But the crystallinity of DBDI based PUs can be also considerably reduced with the incorporation of MDI as earlier reported [61].

In the first step of our study, we have focused our work on the generally employed method of PUs synthesis in the melt, namely the prepolymer route followed by a reaction with a chain extender subsequently cured with air humidity, which consumes all of the isocyanate excess situated on the ends of the intermediary formed active PU oligomer, thereby leading to an additional degree of urea group formation [60]. *In our case, in this study, this referred to a PU synthesized by using a 1 mole of macrodiol – 4 moles diisocyanates – 2.64 moles chain extender system, so to obtain a small isocyanate excess ($I = 110$) situated at the ends of the above active PU oligomer.*

In the PU synthesis we started from one mole of hydroxy-terminated macrodiol which was either a polyester type—polyethylene adipate (PEA) or a polyether type—polytetrahydrofuran (PTHF).

For the preparation of the PU elastomer containing simultaneously two different diisocyanates the macrodiol was reacted in different ways with two moles of MDI and two moles of DBDI. Finally the so-obtained different prepolymers were reacted with 2.64 moles of chain extender which was in all the cases ethylene glycol (EG). There were adopted three different modes of prepolymer synthesis leading to three different active PU oligomers.

- PU_{C1}: Single step prepolymer synthesis which used a melt mixture of the two isocyanates (MDI and DBDI isocyanates). In this case, the two different diisocyanates were inserted more or less randomly into the prepolymer and the resulting full polymer;
- PU_{C2}: A two-step prepolymer synthesis where two moles of DBDI was first reacted with one mole of macrodiol, followed by addition of MDI;
- PU_{C3}: A two-step prepolymer synthesis where two moles of MDI was firstly reacted with one mole of macrodiol, followed by addition of DBDI.

In all cases, it obtained active oligomers with final NCO groups having a calculated molecular weight of about 8 900 [60]. Finally the so-obtained different prepolymers were reacted with 2.64 moles of chain extender which was in all cases EG. There were adopted three different modes of prepolymer synthesis leading to three different active oligomers.

The composition of the PU family prepared in this study is shown in Table 2.2 and the equations are shown in Table 2.3.

Table 2.2 Compositions of the family of polyurethane elastomers prepared and studied in this work

Recipe	PU structure
PU _{C1}	CE ^a –MD ^b –(DBDI–MDI)
PU _{C2}	CE–(MD–DBDI)–MDI
PU _{C3}	CE–(MD–MDI)–DBDI
PU _D	CE–MD–DBDI
PU _M	CE–MD–MDI

^a CE – chain extender; ^b MD – macrodiol

2.3.2.1 WAXS results for polyurethane elastomers with mixtures of diisocyanates. Crystallinity

X-Ray scattering (WAXS) were employed by us on the series of materials labeled in Tables 2.2 and 2.3, in order to follow the changes that were brought about by

Table 2.3 Synthesis routes for PU_C based on mixtures of the diisocyanates MDI and DBDI, with PEA or PTHF as soft phase [60]

PU _{C1} PEA and PU _{C1} PTHF type synthesis		
Single step prepolymer synthesis using a melt mixture of the two isocyanates (MDI + DBDI).		
MD + (2 MDI + 2 DBDI) melt mixture	→	U*~U* + 2 (x MDI + y DBDI) prepolymer U
[U*~U* + 2 (x MDI + y DBDI)] + 2,64 CE	→	OCN U*[G(UG) _{1.64} U~U] _{2.77} NCO
PU _{C2} PEA and PU _{C2} PTHF type synthesis		
Two step prepolymer synthesis where DBDI is first reacted, followed by the addition of MDI.		
MD + 2 DBDI	→	M*~M* prepolymer (M)
[M*~M* + 2 MDI] + 2.64 CE	→	OCN D*[G (DG) _{1.64} M~M] _{2.77} NCO
PU _{C3} PEA and PU _{C3} PTHF type synthesis		
Two step prepolymer synthesis where MDI is first reacted, followed by the addition of DBDI.		
MD + 2 MDI	→	D*~D* prepolymer (D)
[D*~D* + 2 DBDI] + 2.64 CE	→	OCN M*[G (MG) _{1.64} D~D] _{2.77} NCO

MD - macrodiol; CE - chain extender

M* and D* = monourethane-isocyanate sequence derived from monoreacted MDI and respectively DBDI;

M and D = diurethane sequence derived from bireacted MDI and respectively DBDI;

U* and U = mono and respectively diurethane sequence derived from either randomly mono and bireacted MDI or DBDI.

changing the type and the number of isocyanates (one or two diisocyanates), and the order of their introduction in the material synthesis.

As seen in Fig 2.21, for the materials containing *two diisocyanates* of PU_{C1}, PU_{C2} and PU_{C3} types, in both of the soft segments PEA and PTHF, the X-ray diffraction patterns showed in all cases that the crystallinity decreases significantly relative to those with DBDI indicating a decrease of the HS ordering. In general when employing the PU synthesis with mixtures of DBDI and MDI, the crystallinity of the obtained PU decreased relatively the materials obtained by using the diisocyanate DBDI alone. The degree of extinction of crystallinity depended also on the used synthesis route [60].

The crystallinity was considerably reduced with the incorporation of MDI, of which the example of PU_{C1} PEA is presented in Fig. 2.21 (a). In all the PUs containing two diisocyanates, namely PU_{C1}, PU_{C2} and PU_{C3} types with either of the soft segments PEA or PTHF, the X-ray diffraction patterns showed that crystallinity decreases significantly relative to those PUs containing only DBDI (PU_D) indicating a decrease of the HS ordering [60].

To compare more critically the different routes of copolymerization PU_{C1}, PU_{C2} and PU_{C3}, and their effect on the HS ordering, a further WAXS data was collected.

These results major on the PTHF series of materials. With these also, when employing the PUs synthesis with mixtures of DBDI and MDI, the crystallinity was

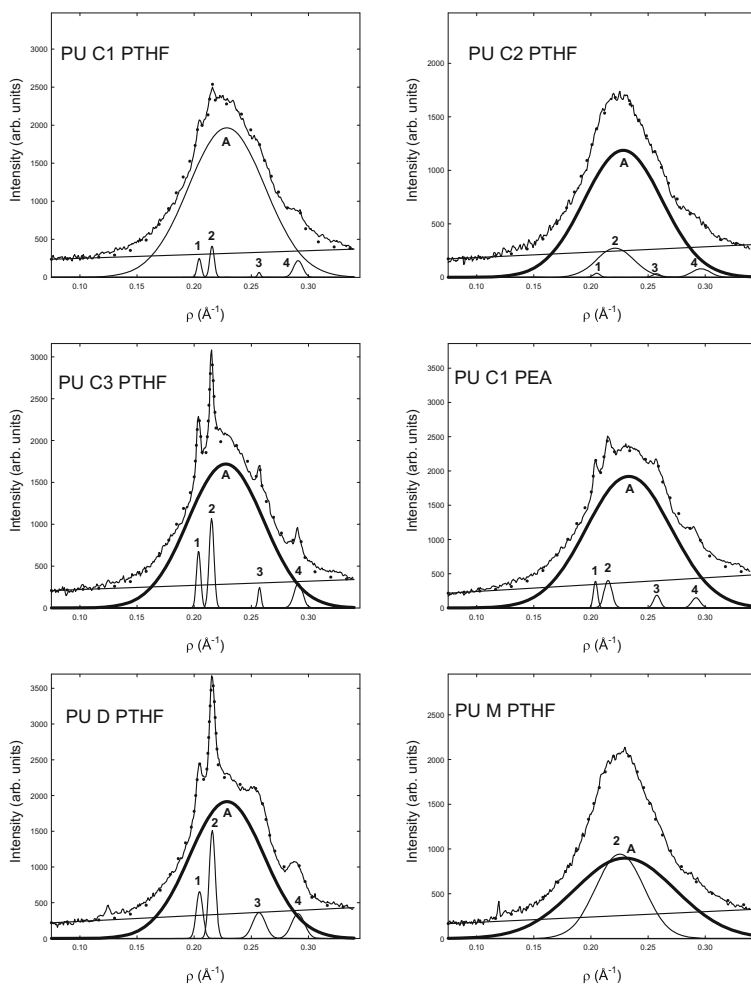


Fig. 2.21 (a) WAXS pattern collected from sample PU_{C1} with PTHF showing the separation of the scattering into crystalline and amorphous components; (b) WAXS pattern collected from sample PU_{C2} based on PTHF showing the separation of scattering components. Here, all the peaks are broad, indicating an amorphous structure; (c) WAXS pattern collected from the PTHF based sample PU_{C3} showing the separation of the scattering into crystalline and amorphous components; (d) WAXS pattern collected from a similar sample type PU_{C1} but based on the macrodiol PEA; (e) WAXS pattern collected from sample based on PTHF and derived from the single diisocyanate DBDI (PU_{D}) showing the separation of the scattering into crystalline and amorphous components. (f) WAXS pattern collected from sample with PTHF derived from the single diisocyanate MDI (PU_{M}) [60].

decreased relative to the unmixed PU_{D} materials, but it is very apparent from Fig. 2.21 that the degree to which crystallinity is depressed depends critically on the synthesis route.

Clearly, the sharp peaks associated with DBDI decreased in the order: $PU_D > PU_{C3} > PU_{C1} > PU_{C2} > PU_M$ corresponding to introduction of DBDI as follows: total polymer:hard segments:mixed:soft segments:none.

The crystallization degree was higher in the case of a polyetheric material of the type PU_{C3} when the introduction in the reaction of DBDI was performed in the second stage, because the HS sequence of the EG-DBDI type becomes preponderant.

Improvement in elastomeric properties, by reducing the crystallinity in PUs based on DBDI, was obtained especially when both diisocyanates were included and reacted together in a random fashion, instead of sequentially by using a pre-polymer stage [60].

It is to be noted that the substitution of the SS from PTHF to PEA did not change the above mentioned conclusions. The WAXS patterns of corresponding pairs based on PEA or PTHF were similar in all cases.

To conclude: X-ray diffraction patterns showed significant crystallisability for the PU materials based on DBDI hard segments. There was evidence of the appearance of more or less complete phase separation associated with the formation of discrete crystalline hard domains. However, when the equimolar mixture MDI+DBDI was used for hard segments (PU type C1) the crystallinity was considerably reduced [60, 61]. As mentioned elsewhere [61], in the case of PU based on the single diisocyanate DBDI, the degree of crystallinity can be reduced also by employing a more flexible chain extender.

As shown [60], a general improvement in PUs properties was obtained after polymer annealing at 160°C for 30 minutes [60] when two diisocyanates (MDI+DBDI) were included in the synthesis at once in a random fashion, i.e. for the type of material PU_{C1} .

By doing this study we believe that new insight has been gained into structure-property relations in polyurethane elastomers by preparing them using mixtures of isocyanates.

2.3.2.2 Morphology of polyurethane elastomers with mixtures of diisocyanates as revealed by SEM

The materials with mixtures of diisocyanates depicted in Tables 2.2 and 2.3 were also investigated by means of SEM [60]. As before, the materials were based on PTHF or PEA.

The structure of these materials contained features at two levels. All the materials displayed a relatively structure on the 10 μ m scale, but which varied considerably from material to material. This is shown in Fig. 2.22 (a)–(f), for the PTHF materials. Of the materials studied in Fig. 2.22, the polymer PU_{C3} PTHF from Fig. 2.22(c) has the coarsest structure while PU_M PTHF has the finest (Fig. 2.22(e)). The materials which display X-ray crystallinity (a, c and d of Fig. 2.22) tend to give a rougher surface morphology than those which do not (b and e of Fig. 2.22). The specimens also show variations in topography such as long scratch marks which derive from

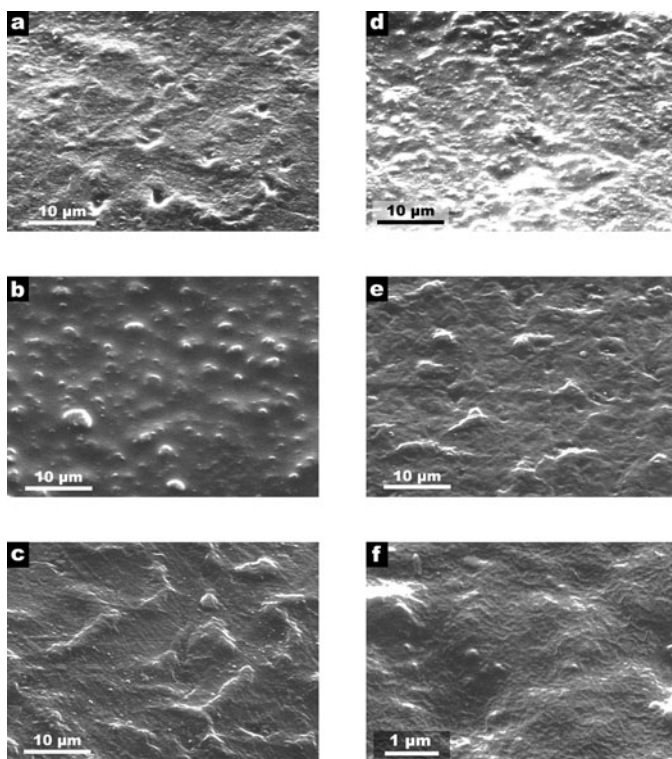


Fig. 2.22 SEM at medium magnification of: (a) $\text{PU}_{\text{C1 PTHF}}$ (b) $\text{PU}_{\text{C2 PTHF}}$ (c) $\text{PU}_{\text{C3 PTHF}}$ (d) $\text{PU}_{\text{D PTHF}}$ (e) $\text{PU}_{\text{M PTHF}}$ (f) SEM at higher magnification showing fine texture of $\text{PU}_{\text{M PTHF}}$ [60]

the PTFE plates against which the sheets were moulded, although we have avoided showing regions where these obscure the characteristic texture of the materials.

There is also a finer texture of scale less than 100 nm, which may correspond to segregation of the two different chemical parts, namely the HS and SS. This is only observed by operating the SEM at higher accelerating voltage and smaller spot size, as in Fig. 2.22 f. Shown here is $\text{PU}_{\text{M PTHF}}$, but finer structure is present in the other materials also. This, however, was not intensively studied, as it would require transmission electron microscopy to give appropriate resolution, and such examination would be better if a suitable chemical etching technique were available to reveal the bulk of the material and remove features associated with the surface.

Several chemical etching techniques were tried by us on these materials [60]. Those based on alkaline reagents (whether potassium hydroxide in alkaline solution, or sodium ethoxide in ethanol) did not react enough even to completely remove the smallest spurious features associated with the moulded surfaces. On the other hand, the permanganic reagent with phosphoric acid gave smooth and uniform attack over all the materials. In Fig. 2.23, etched surfaces of all five materials are shown at three

magnification for easy comparison. $\text{PU}_{\text{C1 PTHF}}$ (Fig. 2.23 a)) shows roundish regions which are raised and therefore more resistant to the etchant, surrounded by a flatish matrix. The scale of these regions is much larger than the length of the HS and SS, so it appears as if some precipitations of one region has occurred during the reaction: in this case the precipitated part is more resistant to etching. The whole surface appears to be strewn with small objects between 0.2 and 0.8 μm in size, which look like crystals whose edges have been rounded off by partial dissolution [60]. It may be that these are a particular chemical species, which has been released by the attack. $\text{PU}_{\text{C2 PTHF}}$ (Fig. 2.23 b)) shows a similar structure, except that the resistant regions are much smaller, although they occupy about the same percentage of the total area. In $\text{PU}_{\text{C3 PTHF}}$ and $\text{PU}_{\text{M PTHF}}$ (Fig. 2.23 c and e), it appears that the relatively resistant material is in the majority, with non-resistant pockets being eaten out by the etchant. It may be that these pockets represent material precipitated during polymerization. In $\text{PU}_{\text{D PTHF}}$ (Fig. 2.23 d)) the overall etched texture is much flatter, so it would seem that the regions of chemical segregation are more or less equally attacked, although what structure there is seems to show a pattern similar to Fig. 2.23 c and e. *Only $\text{PU}_{\text{D PTHF}}$ in Fig. 2.23 d does not show the precipitated crystals: this is the only one of the five examined samples which does not contain MDI, because the crystals are derived from units containing this monomer.* At the highest magnification, there is only a faint suggestion of fine-scale structure such as seen in Fig. 2.23 f, which is most prominent in Fig. 2.23 b (bottom). This particular etchant is therefore not ideally suited to distinguishing between hard and soft segments.

2.3.2.3 Morphology of polyurethane elastomers with mixtures of diisocyanates as revealed by AFM

The morphology of a series of polyester or polyether PUs based on mixtures of diisocyanates has been also examined by ourselves by using the AFM technique. Example PUs that were studied, based on the macrodiol PEA and chain extended with EG are depicted in Table 2.4. The molar composition of the materials was diisocyanate:macrodiol:chain extender = 4:1:3 giving an isocyanate index $I = 100$. The preparation procedures in order to obtain PUs with single or mixtures of the diisocyanates MDI and/or DBDI has been described elsewhere [127, 207].

Normally, the surface of a PU sample fracture shows a relief composed of peaks of HS and crystal aggregates domains. The rupture occurs most probably in the amorphous regions. Therefore, it is expected that such a surface contains more information about the sample morphology than the surface of free solidification or drying. AFM images were taken from different zones for each sample. Shown in Fig. 2.24 are images of freeze fracture surfaces for the whole series of the materials (PU_1 to PU_5).

The values depicted in Table 2.5 for the parameters H_a and S_q show some correlations between the PUs morphology and their chemical structure. Thus, the corresponding roughness order $\text{PU}_2 > \text{PU}_3 > \text{PU}_4 > \text{PU}_1 \approx \text{PU}_5$ shows that the most uneven relief appears when the materials is obtained by the two stage polyaddition

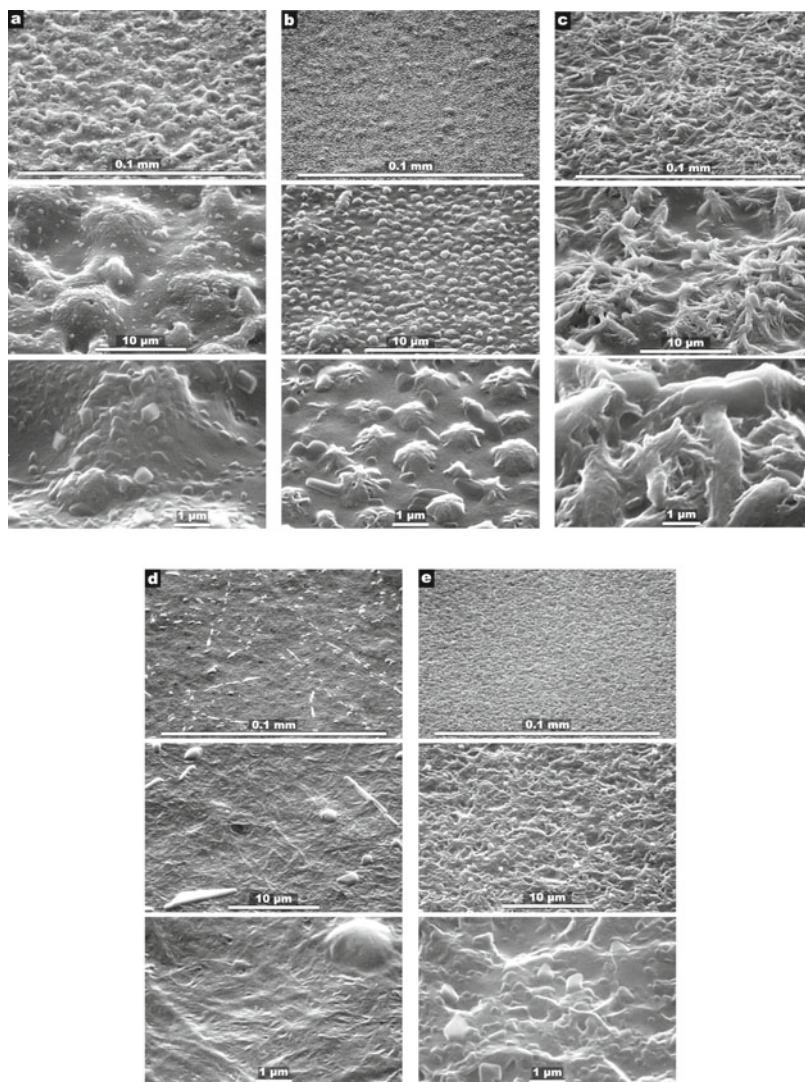


Fig. 2.23 SEM of etched polyurethane specimens at three magnifications: (a) PU_{C1} PTHF; (b) PU_{C2} PTHF; (c) PU_{C3} PTHF; (d) PU_D PTHF; (e) PU_M PTHF [60]

procedure. A plausible explanation would be the following: when the macrodiol is first and completely reacted with one of the two diisocyanates (here denoted as DI₁), the excess of 2 moles of DI₁ to 1 mole of macrodiol in the first reaction step results in a prepolymer that mainly consists of macrodiol molecules with monoreacted DI₁ ends. At the end of the process, when the rest of the reactants is added, (i.e. 3 moles of chain extender and 2 moles of the second diisocyanate (here denoted as

Table 2.4 Compositions of the family of PUs [207]

Recipe	PU structure	PUs composition			
		Moles of PEA	Moles of MDI	Moles of DBDI	Moles of EG
PU ₁	EG-PEA-(DBDI-MDI)	1	2	2	3
PU ₂	EG-(PEA-DBDI)-MDI	1	2	2	3
PU ₃	EG-(PEA-MDI)-DBDI	1	2	2	3
PU ₄	EG-PEA-DBDI	1	0	4	3
PU ₅	EG-PEA-MDI	1	4	0	3

(DI₂)), a polymer with $-(DI_2-CE-DI_1-MD-DI_1-CE-DI_2-CE)-$ units should result (where CE is the chain extender). This is the case with the polymers PU₂ and PU₃.

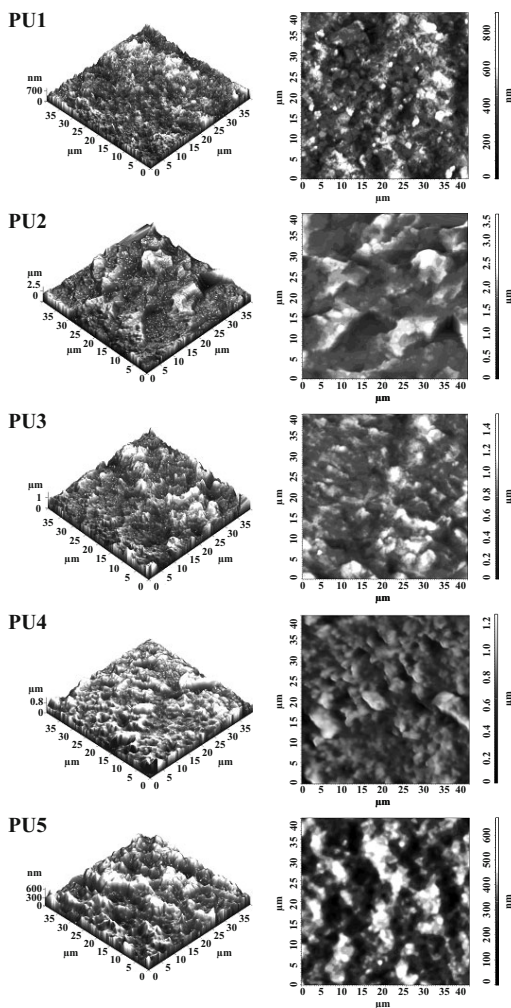
Table 2.5 Surface roughness parameters from AFM height images [207]

Sample identification		Crystallinity index [135]	Surface roughness parameters		
Code	Composition	CI (%)	H _a [nm]	S _q [nm]	NSH (H _a /S _q)
PU ₁	EG-PEA-(DBDI-MDI)	<20	399.4	116.1	3.44
PU ₂	EG-(PEA-DBDI)-MDI	>20	1617.7	368.9	4.38
PU ₃	EG-(PEA-MDI)-DBDI	>30	717.4	191.8	3.74
PU ₄	EG-PEA-DBDI	~50	669.3	153.9	4.35
PU ₅	EG-PEA-MDI	>25	320.1	101.6	3.15

The fact that the roughness is significantly higher for PU₂ than for PU₃ may be associated with the crystallinity, which is promoted by the presence of DBDI and is absent in the materials based on the single diisocyanate MDI (Table 2.5). The difference in crystallinity associated with DBDI and MDI was previously evidenced and ascribed to the flexibility of the hard segments, which is characteristic to the DBDI segments and absent in the MDI hard segments [127].

Regarding the roughness order, it is evident that the cross sections of the materials PU₄, PU₅ and PU₁ (where the two diisocyanates are mixed together at once in a random fashion via the one stage prepolymer synthesis route) are smoother than those obtained by the two stage prepolymer polyaddition procedures. This is not only due to crystallinity as long as this parameter is the largest for the materials PU₄, and not for the polymer PU₂. Taking into account the morphology model of the HS phase dispersed into the SS phase proposed by Christenson et al [208], our assumption was that the domains of the SS crystals joined by the HS matrices are small and dense in the PUs obtained by the one step prepolymer route, while they are bulky and rare in the PUs obtained by the two step prepolymer techniques. Such a morphology is supported by the topographic 3D and 2D images shown in Fig. 2.24

Fig. 2.24 Tapping mode AFM topographic 3D and 2D images for freeze fracture surfaces for materials listed in Tables 2.4 and 2.5 [207]



if, for example, the images of the samples PU₂ and PU₅ are compared with those of the samples PU₂ and PU₃, respectively.

It results that the different morphologies are related to the differences in the chain microstructure. Therefore, while the chains resulted from two step prepolymer syntheses, are predominantly built with $-(DI_2-CE-DI_1-MD-DI_1-CE-DI_2-CE)-$ units, the chains obtained from one step prepolymer polyaddition processes are more heterogeneous due to the presence of amounts of other sequences like $-CE-DI-MD-DI-MD-DI-$ and $-CE-DI-CE-DI-CE-DI-$. Obviously, the polymer chain heterogeneity does not promote the orientation of the chains.

It is of interest to consider the NSH parameter given by the ratio of the average height, H_a , to the RMS roughness, S_q . Discussion about this parameter is absent in the literature. As shown in Table 2.5, the NSH follow the order of the values of H_a

and S_q , but the differences between the materials are smaller. By correlating NSH with the characteristics of the surface relief it observed that NSH increased not only with the roughness, but also with the decrease of the relief uniformity. Comparing the materials PU₄ and PU₂, which showed much different values for H_a and S_q , but almost similar NSH values, it resulted that the relief of the material PU₂ is more uniform than that of the polymer PU₄.

The AFM images of fracture surfaces revealed that the PUs obtained by the two stage prepolymer poliaddition provedure, have a more uneven relief than the those of the material obtained by the one step prepolymer technique. In addition, DBDI increases this difference, but leads to more uniform relief forms than does MDI.

Polyurethane Elastomers
From Morphology to Mechanical Aspects
Prisacariu, C.
2011, XXIV, 255 p., Hardcover
ISBN: 978-3-7091-0513-9